PERGAMON

Journal of Structural Geology 25 (2003) 171–182

JOURNAL OF STRUCTURAL GEOLOGY

www.elsevier.com/locate/jsg

Interpreting anomalous magnetic fabrics in ophiolite dikes

G.J. Borradaile*, D. Gauthier

Geology Department, Lakehead University, Thunder Bay, Ontario, Canada P7B 5E1

Received 24 July 2001; received in revised form 15 November 2001; accepted 31 January 2002

Abstract

Anisotropy of magnetic susceptibility (AMS) may reveal mineral orientation-distributions defining magmatic flow-axes in igneous dikes. The mafic silicates are the best indication of magmatic flow but Fe–Ti accessories may contribute more to the bulk susceptibility. If the orientation-distributions of the two subfabrics are incongruent, anomalous fabrics will occur that do not reflect magma-flow axes. For ophiolite dikes, ocean-floor metamorphism changes the mineralogy producing new Fe-oxides by retrogression and exsolution from mafic silicates and by the oxidation of primary oxides. Incompatibly oriented 'ferro'-magnetic subfabrics may be isolated by anisotropy of anhysteretic remanence (AARM). Anomalous AMS fabrics in ophiolites elsewhere have been attributed to inverse-fabric contributions from single-domain magnetite in varying combinations. However, in ophiolite dikes from the Troodos ophiolite of Cyprus, anomalous fabrics arise from ocean-floor metamorphism extensively or completely replacing the original magnetite and titanomagnetite accessory phases with titanomagnetite ($\sim Fe_{2.4}Ti_{0.6}O_4 = TM60$) and its oxidised versions, titanomaghemite, to varying degrees according to depth beneath the ocean-floor, distance from spreading axis and proximity to transform-faults. At best, the oxide orientation-distribution defined by AARM could only be indirectly related to magma-flow if its nucleation-orientation controlled by a host-lattice. However, more commonly the topotactic lattice reorganization produces weaker ARM fabric anisotropies. Although 'recrystallized', oxidised TM60 dominates the *bulk* low-field susceptibility, its anisotropy is generally too feeble to compete with the flow-fabric defined by the AMS contribution from paramagnetic mafic silicates.

Keywords: Ophiolite dikes; Anisotropy of magnetic susceptibility (AMS); Mafic silicates

1. Introduction: magnetic fabrics and magnetic mineralogy

Magmatic flow directions in dikes are constrained by the dikes' walls but petrofabric investigation is required to determine the axis of flow or direction of flow, and the relative importance of linear and planar mineral-orientation-distributions. It is now well accepted that magnetic anisotropy yields the most efficient and representative petrofabric orientation-distributions. Where the anisotropy of low field magnetic susceptibility is measured (AMS), the contributions of minerals with diamagnetic, paramagnetic and 'ferro'-magnetic responses merge, giving an overall tensor, represented by an ellipsoid (axes k_{MAX}, k_{INT}, k_{MIN}) that in some way corresponds to the orientation-distribution of mineral grains (Hrouda, 1982; Borradaile, 1988; Hrouda and Schulmann, 1990; Borradaile and Henry, 1997). To this end, we sampled seven dikes at two sites yielding 43 oriented-blocks and 139 right-cylindrical core samples (25 mm diameter × 22 mm high) from the eastern part of the Troodos sheeted dike complex in Cyprus (Fig. 1). These ophiolite dikes formed near a spreading-axis in the Tethys ocean and the orientation of magma-flow axes may give the relative location of magma chambers, whose size and spacing may permit estimates of the relative ocean-floor spreading-rate (Detrick et al., 1990; Dilek et al., 1998). Previous studies followed the simple but reasonable premise that AMS alone may uniquely define the flow-axis and flow-foliation (Rochette et al, 1991a,b; Staudigel et al., 1992, 1999) or, with more work and suitable outcrop, that imbricate AMS-foliations along dike margins isolate the flow-axis (also the direction; e.g. Knight and Walker, 1988; Varga et al., 1998). Whereas such studies have been very successful in relatively fresh basaltic lava and dikes in non-tectonized and non-ophiolitic environments (Elwood, 1978; Ernst and Baragar, 1992; Knight and Walker, 1988), our fabrics are more difficult to interpret, comparable with those found by Rochette et al. (1991a,b, 1992, 1999). This we attribute to the fact that the ophiolite dikes underwent significant sea-floor hydrothermal metamorphism creating a post-magmatic Fe–Ti oxide assemblage characterized by the replacement of the primary assemblage of magnetite

* Corresponding author. Tel.: +1-807-343-8461; fax: +1-807-935-2753.
E-mail addresses: borradaile@lakeheadu.ca (G.J. Borradaile), dave@ freedomcomputing.com (D. Gauthier).

0191-8141/02/$ - see front matter
PII: S0191-8141(02)00025-1

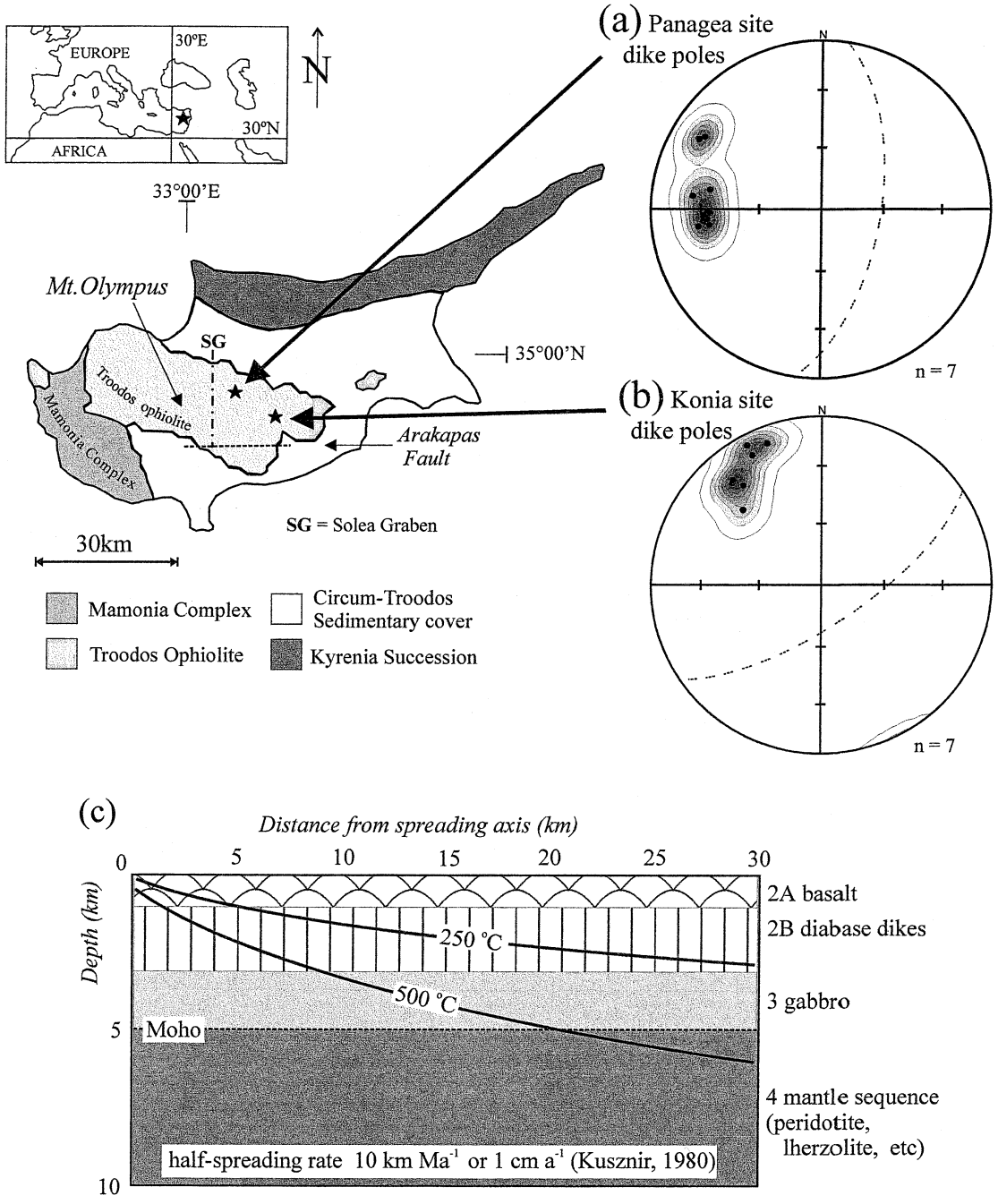

Fig. 1. Location of the two sites in the sheeted dike complex of the Troodos ophiolite of Cyprus. The earliest spreading axis was associated with the Solea Graben (SG). A fossil transform marked as the Arakapas Fault modified dike and fabric orientations in the SW portion of the ophiolite. Lower hemisphere equal area projections with contours in multiples of expected uniform density using the program Spheristat by Pangea Scientific. (a) Poles to dikes at Pangea. (b) Poles to dikes at Konia. (c) Idealized oceanic crust-mantle profile showing theoretically determined isotherms adjacent to a spreading axis with half rate of 10 km Ma^{-1} from Kusznir (1980). The spreading rate of the Troodos ophiolite may have been at least 20 km Ma^{-1} implying that the isotherms may not have been as depressed as shown here.

and $Fe_{2.4}Ti_{0.6}O_4$ ('TM60') with more oxidized versions (titanomaghemite). We shall demonstrate that despite the oxide-subfabric's high bulk susceptibility, its anisotropy is relatively low compared with that of the silicate matrix so that, nonetheless, AMS axes approximate flow-axes.

First, let us review some elements of magnetic mineralogy. In the presence of a magnetic field, certain minerals such as pure feldspars, calcite and quartz yield a feeble diamagnetic response that is mostly negligible in comparison with the overwhelming response of even low concentrations of paramagnetic or ferromagnetic grains. In the dike rocks we describe, paramagnetic minerals, such as pyroxene, olivine, serpentine and chlorite make a significant contribution to AMS and also define the petrofabric which

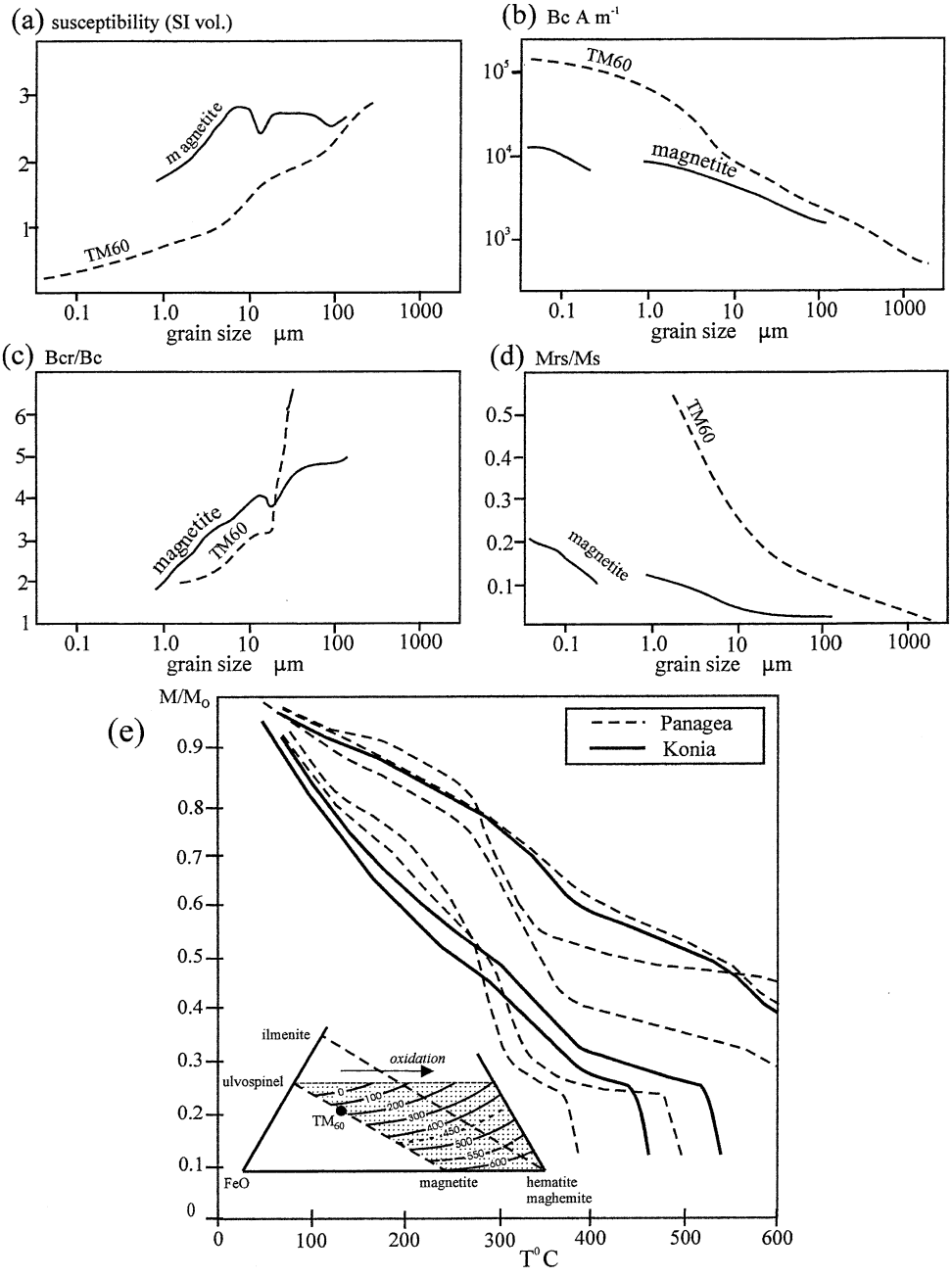

Fig. 2. (a–d) Rock magnetic properties of magnetite compared with $Fe_{2.4}Ti_{0.6}O_4$ ('TM60'), generalized from O'Reilly (1984). B_c = coercive force; B_{cr} = coercivity of remanence; M_{rs} = maximum remanence in zero-field; M_s = saturation remanence under applied field. (e) Curie temperatures on heating typical dike-samples in this study. Inflection points near ~250 °C may be due to TM60, but the most prominent inflection points ~300–325 °C suggest more oxidized versions such as titanomaghemite. Traces of magnetite are indicated by Curie points ~580 °C. (Inset ternary diagram with Curie-temperatures after Dunlop and Özdemir, 1997; O'Reilly, 1984.)

is due to magmatic flow alignment in most cases. However, the silicate alignment is subtle and difficult to measure in three dimensions. If the AMS was entirely due to the silicates it would provide the orientations of the principal axes of an average orientation-distribution anisotropy. Of course, that common assumption is an approximation since each mineral has a different AMS which is rarely coaxial with crystallographic axes. Following Neumann's principle the symmetry elements of any anisotropic physical property, including AMS, must *include* the symmetry elements of the crystal (Nye, 1958). The dikes' mafic silicates are monoclinic and thus one crystallographic axis will be parallel to a principal susceptibility value (Borradaile and Werner, 1994; Lagroix and Borradaile, 2000). There is no direct, simple one-to-one correspondence of crystal axes' orientations (or dimensions) with the axes of the grain's AMS ellipsoid unless the crystal is of high symmetry (e.g. orthorhombic). At best, the orientation-distribution of AMS axes of a

polycrystalline sample may only be taken as an approximate indication of the axes of the orientation-distribution of paramagnetic silicates. Whereas the correspondence of principal directions may be debatable, the relative magnitudes of the AMS axes is quite misleading in terms of the shape of the orientation-distribution ellipsoid. (Further extrapolations to the symmetry, magnitudes or tensor-ellipsoid-shapes of causative processes or phenomena such as stress, strain or flow appear even more highly optimistic.)

At an early stage in magnetic fabric work, it was realized that anomalous fabrics could arise for certain minerals (e.g. tourmaline, calcite; Owens and Rutter, 1978; Rochette, 1988; Rochette et al., 1992) where a long-dimension of a crystal corresponds to a minimum susceptibility axis, or vice-versa. Single-domain magnetite (SD) produces a similar 'inverse fabric effect', for a very different reason, as explained below. This leads us to the subject of the Fe–Ti oxide accessories.

The presence of iron oxides in the dikes is obvious, typically ranging from 1 to 5% by volume, which largely accounts for the high susceptibilities of many dikes, usually >20,000 μSI. The theoretical maximum susceptibility contribution of a mafic silicate is ~2000 μSI so that the dike's bulk susceptibilities must be due to accessory oxides or oxide inclusions in silicates. Thermomagnetic tests detect Curie-points appropriate for magnetite and titanomagnetite (~TM_{60}), but mainly the oxidised version, titanomaghemite (Fig. 2e), by comparison with published information (O'Reilly, 1984; Dunlop and Özdemir, 1997). In the common grain-sizes, titanomaghemites have mean susceptibilities ~0.5 SI approximately 100 times that of our ophiolite dikes (Dunlop and Özdemir, 1997, fig. 3.19). Thus, the susceptibility of a few percent oxide may equal or exceed that of the matrix. Nevertheless, oxides need not mask the *anisotropy* of the less susceptible silicate matrix whose paramagnetic-anisotropy and alignment are usually stronger (Borradaile, 1987).

Both primary and secondary oxides of sub-oceanic basic rocks depend on depth and an extensive discussion is found in Dunlop and Özdemir (1997). Near the top of the basic rock-sequence, primary TM60 is found, whereas at greater depths magnetite predominates. Hydrothermal metamorphism replaces TM60 with titanomaghemite, less so at greater depths and at the greatest depths it may invert to magnetite and ilmenite. The mafic silicates may also exsolve magnetite during sea-floor metamorphism. Thus in sheeted dikes, one may expect dominantly secondary minerals forming the Fe–Ti oxide accessory assemblage among which titanomaghemite, magnetite and ilmenite are expected. Ilmenite has high susceptibility like titanomagnetites but, as with TM(>80), it does not carry a remanence at ambient temperatures and is therefore invisible to AARM.

In the context of magnetic fabrics, our general preoccupation is with magnetite, hematite or ilmenite that respond differently or not at all to studies by AMS and AARM. Unfortunately, oxides in ophiolites have more complicated mineralogy and history. Mineral-magnetic properties that have a bearing on measurement and interpretation of AMS and AARM are reviewed below in as far as they influence measurements of AMS, AARM and the interpretations of the orientation distribution of the oxides. Their preferred orientation is expected to be weak or nearly uniform for two reasons. First, the solid state growth does not occur in rocks accumulating finite strain. Second, growth may be by internal crystallographic rearrangements of existing grains or exsolution from silicate hosts. Thus despite the high mean-susceptibilities of ophiolite oxides, they are not expected to overpower the rock's AMS.

Trends in behaviour accompanying the replacement of primary oxides by titanomaghemite in ophiolite dikes may be inferred from comparisons of magnetite and TM60 (O'Reilly, 1984), here summarized in Fig. 2a–d. TM60 does not replace magnetite in ophiolites, rather titanomaghemite replaces magnetite and TM60 so the following comments merely indicate possible general tendencies. First, bulk susceptibilities are lower than magnetite, more so in the finer grain-sizes (Fig. 2a). At common concentrations, TM60 would dominate the *bulk* susceptibility of the metamorphosed rock. Secondly, the coercive force (B_c, the *active* magnetic field required to oppose the remanence) is much higher than for magnetite, though much less so for the largest, visible grain-sizes (Fig. 2b). Below, we shall see that the difficulty of erasing or applying a remanence is important in understanding the anisotropy of remanence. Thus, thirdly, we must appreciate how difficult it is to erase a magnetic memory permanently. This is expressed as coercivity of remanence: the field (B_{cr}) required to neutralise a remanence so that it is absent even when the opposing field is removed. It is conveniently normalised to coercivity; thus B_{cr}/B_c indicates the 'tenacity' of remanence. TM60 production reduces B_{cr}/B_c for smaller grains but increases it considerably for large multidomain (MD) grains, i.e. >20 μm (Fig. 2c). Finally, the success of potential remanence preservation is changed by sea-floor metamorphism. This is conveniently expressed by normalising M_{rs}, the maximum possible remanence intensity in zero-field (i.e. ~earth's field) to M_s, the saturation magnetisation in the presence of a suitably large applied field. Thus, M_{rs}/M_s represents an idealised potential remanence intensity, all other factors being equal. The replacement of magnetite by TM60 would produce an increase in M_{rs}/M_s, especially in finer grain-sizes (Fig. 2d).

Replacement Fe–Ti accessory minerals not only change the bulk susceptibility and remanence properties of the rock; they also change the orientation of susceptibility axes. The Fe–Ti oxides are not part of any primary flow-fabric in the silicate matrix. Although they may form mimetically on an earlier, flow-oriented lattice that would not necessarily enhance the pre-existing alignment (Borradaile, 1994; Borradaile and Werner, 1994; Lagroix and Borradaile, 2000). Moreover, most probably form topotactically, by complex

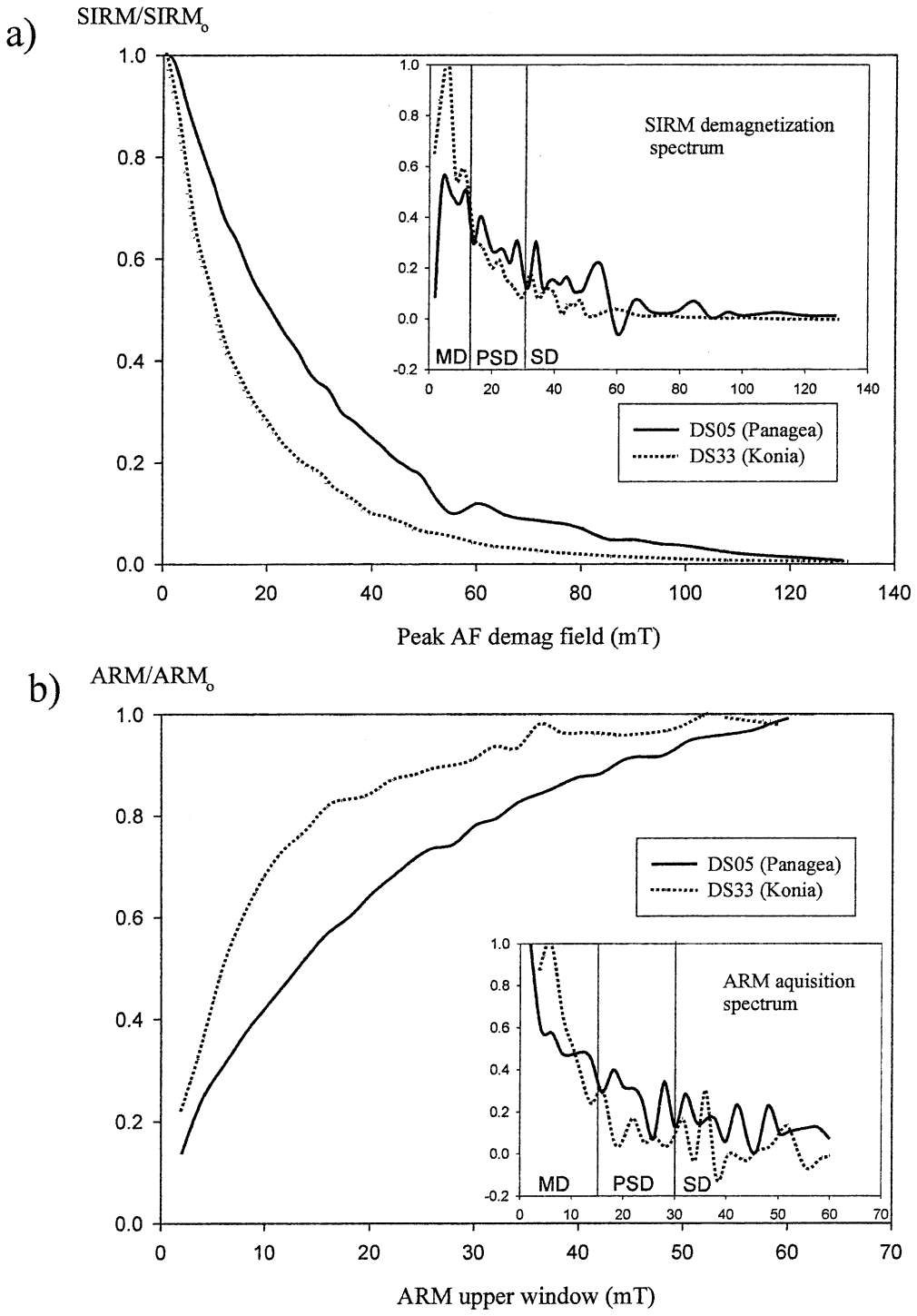

Fig. 3. (a) Alternating field (AF) demagnetization of isothermal remanence (IRM) acquired at 1.0 Tesla. Inset spectrum of coercivity-of-remanence (B_{cr}) and, for comparison only, domain-state-ranges commonly reported for *magnetite* (MD = multidomain, PSD = pseudo-single domain, SD = single-domain). (b) Intensity of anhysteretic remanence (ARM) acquired with successively higher upper window-frame for the AF over which the DC bias field was applied. In all cases, the *peak* AF was 180 mT and the DC field was 0.1 mT as in the experiments in which anisotropy of ARM was measured (Figs. 4 and 5).

lattice-shuffling of pre-existing grains. It is improbable that even a strong preferred orientation of oxides could be preserved by their pseudomorphs that would in any case probably possess non-unique polycrystalline AMS. It is probably partly for these reasons that some ophiolite AMS fabrics are difficult to reconcile with primary magmatic flow fabrics.

Therefore, it is useful to isolate the oxide subfabric orientation-distribution using a different magnetic anisotropy technique. Since magnetite and most of the oxidised Ti–Fe oxides

(e.g. TM[<80]) *retain* magnetism at ambient temperatures after the removal of an applied field, we have determined the anisotropy of *remanent* magnetism. An artificial remanence was applied in the laboratory using an anhysteretic remanent magnetization (ARM) which has the advantage that the permanent-ordering occurs in a weak DC field (0.1 mT). To produce a measurable intensity, the sample is exposed to the DC field during the decay of a large alternating field (from 180 mT down to zero). The AF mobilizes the moments so that as it changes sign during its sinusoidal decay, the small DC bias field aligns certain moments. The ARM is applied in different orientations through the sample and measured after application. From the different permanent magnetizations in different directions one may calculate the tensor of anisotropy of remanent magnetization, in a manner analogous to the determination of AMS by induced fields (see Jackson (1991) for AARM; Daly and Zinsser (1973) and Jelinek (1993, 1996) for IRM anisotropy). One complication is that one must ensure that each successive step in the AARM procedure overprints the preceding ARM. This could be done using three-axis AF demagnetization between each ARM-application but we devised a sequence of orientations in which each subsequent ARM application is at a non-orthogonal angle to the previous ARM, thereby demagnetizing it. This scheme has been tested on numerous occasions in materials of varying coercivities. Moreover, during each AARM experiment it is simple to verify the correct application because the ARM direction should be parallel to the direction in which the field was applied. The orientation scheme for measurement axes is the same for our AMS measurements (seven-orientation system of Borradaile and Stupavsky, 1995). Since ARM requires the application of a weak DC field during AF demagnetization, it is only applicable to minerals with reasonably low coercivity, such as magnetite. It is also more successful if the Curie temperature is considerably above room temperature. For these reasons, our ophiolite dikes do not give very strong ARM signals. With the DC field of 0.1 mT only ~40% of our AMS samples had sufficiently strong ARM intensities to yield reliable anisotropy measurements.

Thermomagnetic tests (Fig. 2) revealed that the magnetic mineralogy is probably dominated by Ti–Fe oxides. However, TM_{60} is reported with Curie temperatures in the range 150–220 °C (O'Reilly, 1984; Fig. 5), whereas our thermomagnetic test only show feeble inflexion points in this range. On heating, our samples have clearer Curie temperatures in the range 300–350 °C, which correspond to reported values for oxidized TM_{60} (Fig. 5) and some >560 °C corresponding to residual magnetite (magnetite produced during cooling is due to inversion). Oxidised TM60 may have susceptibilities to contribute significantly to AMS but their known coercive forces and coercivity of remanence are not so high that they are unsuitable for the measurement of AARM. Therefore, AARM may successfully isolate the orientation-distribution of these accessory phases. However, we may expect subfabric-contributions from primary magnetite, early TM60 as well as its oxidation products. Samples were only rejected for AARM measurement if the remanence intensity was too low or if the magnetic moment was too heterogeneously distributed in the measurement-cores. Finally, one should note that AARM must be measured after AMS, because the application of large AF may change the low-field susceptibility and AMS of multidomain iron oxides (Potter and Stephenson, 1990).

How do the oxides contribute to ARM and to AMS? We examined typical samples from the two sites using AF demagnetization of saturation isothermal remanence (SIRM) and acquisition of ARM to yield the curves of Fig. 3. Saturation isothermal remanence acquisition was imposed in a Sapphire Instruments SI-6 pulse-magnetiser at 1.0 Tesla. Its intensity was then re-measured after each step of AF-demagnetization in a Sapphire Instruments SI-4 demagnetizer. Differentiating this cumulative curve manually then yields a remanence-coercivity (B_{cr}) spectrum that indicates proportions of IRM carried in different ranges (Fig. 3a, inset). (The domain-state ranges for B_{cr} in the insets of Fig. 3 are for *magnetite* and are for comparative purposes only.)

ARM was acquired using a DC bias field of 0.1 mT and a *peak* alternating field of 180 mT. The DC bias field was applied over AF-windows of different sizes, with the lower limit set at zero. Thus, the first ARM was applied over an AF window of 2.0 mT to zero and its intensity was measured. Subsequent, larger ARMs were acquired in the same direction in the sample, using larger windows, e.g. upper limit set at 4, then 6, then 8 mT…etc. Differentiating the cumulative intensities or acquisition curves of Fig. 3 yields remanence-coercivity (B_{CR}) spectra.

Demagnetization of SIRM shows most remanence is carried in the remanence-coercivity range 0–15 mT, and slightly less in the range 15–30 mT (Fig. 3a). These would correspond to *magnetite* grain behavior that is, respectively, multidomain (MD) and pseudo-single domain (PSD) in character. Thus, by comparison with magnetite, AMS fabrics may preferentially include contributions from the alignment of larger oxide grains. SD-magnetite grains do not contribute significantly to remanence and it is unlikely that there are 'inverse' fabric contributions to AMS. ARM-acquisition indicates that most remanence of that type is acquired over remanence-coercivity-windows corresponding to ranges for MD *magnetite*. The AARM fabrics may therefore largely reflect the orientation-distribution of larger oxide grains. The foregoing inferences from the spectral graphs of SIRM (Fig. 3a) and of ARM (Fig. 3b) involve some leaps of rock-magnetic faith, not least of which is the appropriateness of transferring well-known domain-structure associations of magnetite to the less well understood and probably much more complex Fe–Ti oxide domain-structure (O'Reilly, 1984; Dunlop and Özdemir, 1997).

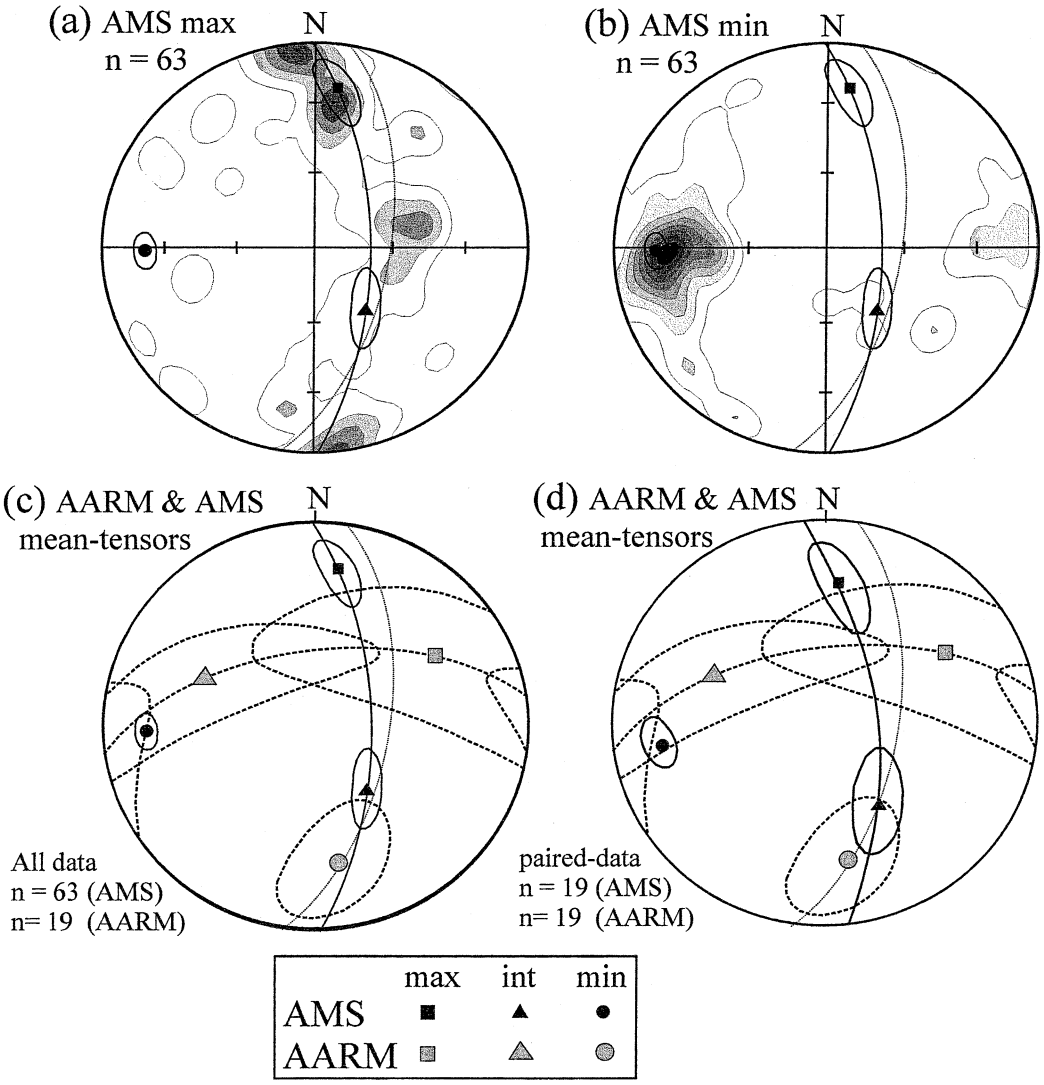

Fig. 4. Magnetic fabric data from the northern site, Panagea, furthest from the E–W Arakapas Transform fault zone (Fig. 1). Dotted plane is mean dike orientation. All stereograms are equal area, lower hemisphere with mean axes for the orientation-distribution tensor (Jelinek, 1978) shown by squares (maxima), triangles (intermediate) and circles (minima); 95% confidence cones about the mean axes are shown. Contours in multiples of expected uniform distribution from Spheristat software (Pangea Scientific). (a) Contours of. AMS maxima. (b) Contours of AMS minima. (c) Mean axes and confidence cones for AMS (solid lines, solid symbols) compared with AARM (dashed lines, gray symbols).

Magnetite is unique in that its induced magnetic response in AMS corresponds to its *grain-shape*. Thus, magnetite does not present the problem of non-correspondence between crystallographic and susceptibility axes as shown by most rock-forming silicates. However, the one-to-one correspondence of AMS with the preferred dimensional orientation is valid only for MD magnetite. In SD magnetite, spontaneous magnetization is fixed by the long and 'easy' axis of magnetization. Therefore, no further magnetization can be induced parallel to the long axis of a monodomainal magnetite grain and it appears as the axis of lowest susceptibility (k_{MIN}) in an induced field when measuring AMS (Stephenson et al., 1986; Potter and Stephenson, 1988, 1990; Jackson, 1991; Rochette et al., 1992). Consequently, SD magnetite yields 'inverse fabrics' in AMS.

AARM isolates the fabric contribution of remanence-bearing accessory grains and ignores the paramagnetic contribution, i.e. the contribution of the matrix-silicates. Its tensor is therefore usually simpler to determine because it is due to fewer mineral species, and also to accessories that developed at a different time and over a shorter interval than the matrix. Moreover, the 'inverse' effect shown by SD magnetite in AMS disappears with AARM, so that the AARM tensor images the orientation-distribution of magnetite grain-shapes or preferred lattice orientations of other Fe–Ti oxides.

In general, we perceive AMS as a complex summation of the orientation-distribution of matrix grains of multiple minerals with different crystal-symmetry control on crystal-AMS, onto which is superimposed a contribution from high-susceptibility accessories or remanence-bearing grains. Although the latter fabric can be isolated by

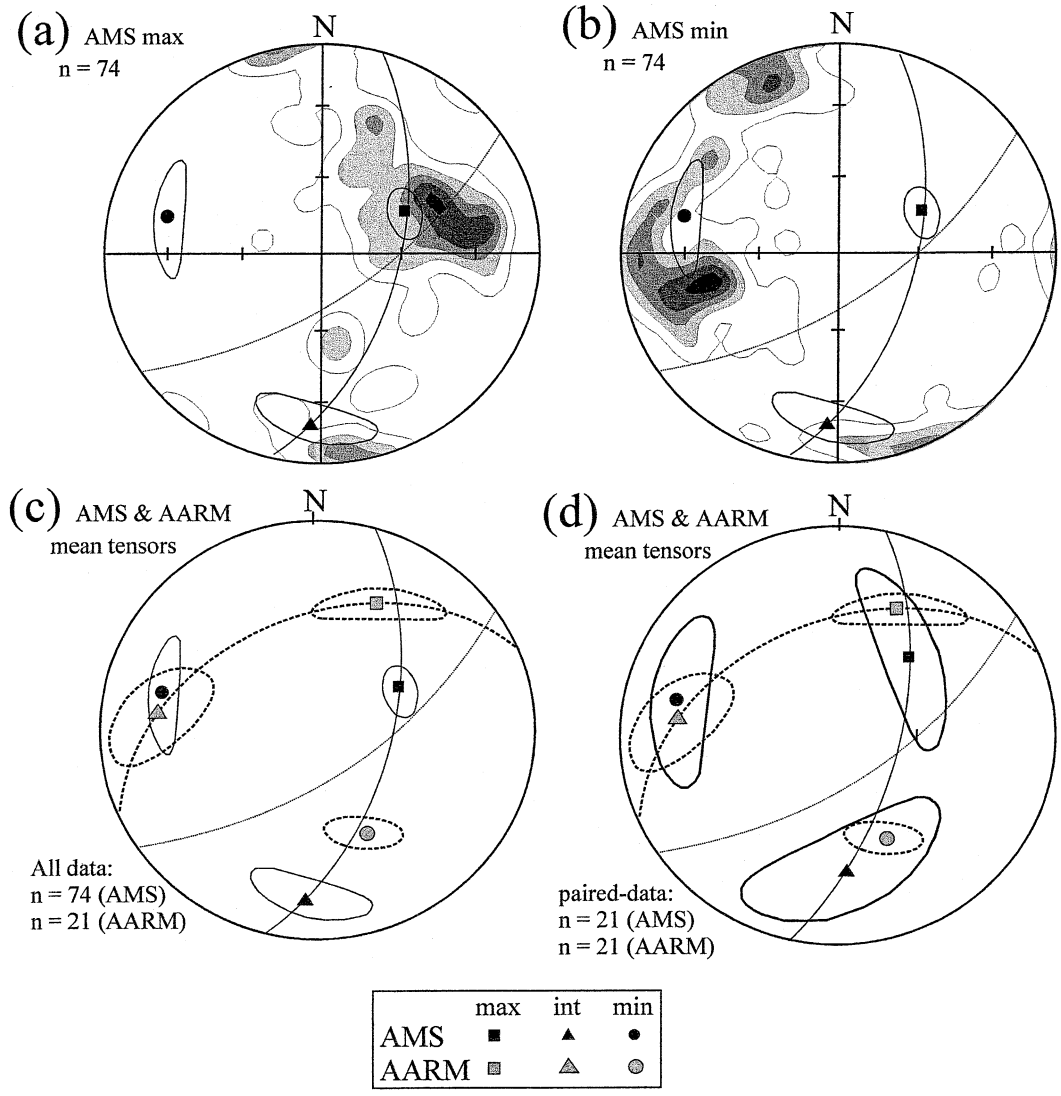

Fig. 5. Magnetic fabric data from the southern site, Konia, closest to the E–W Arakapas Transform fault zone (Fig. 1). Dotted plane is mean dike orientation. All stereograms are equal area, lower hemisphere with mean axes for the orientation-distribution tensor (Jelinek, 1978) shown by squares (maxima), triangles (intermediate) and circles (minima) with 95% confidence cones about the mean orientations. Contours in multiples of expected uniform distribution from Spheristat software (Pangea Scientific). (a) Contours of AMS maxima. (b) Contours of AMS minima. (c) Mean axes and confidence cones for AMS (solid lines, solid symbols) compared with AARM (dashed lines, gray symbols).

AARM, it is extremely difficult to subtract it from AMS in order to determine the 'matrix-only' contribution in AMS (Borradaile et al., 1999; Hrouda et al., 2000).

The mineral orientation-distributions that we infer from AMS and AARM are due to flow-fabrics in dikes complicated by sea-floor alteration and transform-fault shearing. Our approach was to measure a large number of samples from structurally homogeneous sites with suitably fine-grained rocks to provide representative core-samples. Dike centres were sampled to avoid possible imbricate dike-margin fabrics. A careful comparison of both anisotropies with dike-orientations may under these circumstances be productive. Rochette et al. (1992) showed how AMS-interpretation of aligned silicate lattices and magnetite grain-shapes were further comfounded by 'inverse' contributions from SD magnetite. In the unlikely event that SD magnetite dominated the AMS signal, one would indeed see a perfect inverse fabric with k_{MIN} parallel to the magnetite alignment and 'petrofabric' alignment. More commonly, a blended fabric arises in which the inverse component from accessory monodomainal magnetite competes with a normal component from the matrix to produce some mixed fabric that may be difficult to interpret. The magnitudes of the samples' net AMS axes may not correspond correctly to the magnitudes of, e.g. strain or stress. Still worse, the samples' AMS axes may not even be parallel to significant kinematic or petrofabric axes. Rochette et al. (1992) term these 'intermediate' fabrics but we prefer to describe them as blended or mixed to avoid any confusion with a discrete orientation axis or specific 'middle' scenario that may arise in this context. In

the Troodos ophiolite dikes, it appears that greater complications arise from the crystallographic orientation-distributions of TM60 and its oxidised replacements.

2. Discussion of fabrics

Our two structurally homogeneous sites lie within the SE portion of the Troodos ophiolite dike swarm of Cyprus (e.g. Varga et al., 1998). At Panagea, we determined AMS for 63 samples and AARM for 19 samples from seven undeformed dikes (Fig. 4). At Konia, the dikes are closer to a fossil transform fault, which caused dextral transpression and cataclastic deformation. The dikes are pervasively sheared and show a trend different from the general N–S primary strike (Fig. 1a and b). There we measured AMS of 74 samples and AARM of 21 samples from seven non-pervasively sheared dikes at each site (Fig. 5). We tested compared samples from dike walls and dike centres from sections through individual dikes but found no convincing evidence for imbrication of magnetic foliations that might yield flow-axes and directions although that has been effective in other studies elsewhere (MacDonald and Palmer, 1990; Jackson and Tauxe, 1991; Staudigel et al., 1992; Canon-Topia et al., 1994; Palmer and MacDonald, 1999). Dike margin fabrics are visibly more heterogeneous, have less stable fabric orientations, show effects of grain size variation and differing degrees of alteration. Therefore, we sampled dike centres to provide the most consistent fabrics and potentially more reliable information on magma flow-axes.

The non-deformed Panagea site provides an AMS pattern that is readily interpretable following conventional wisdom. North–South, near vertical dikes are almost parallel to the AMS foliation (defined by k_{MAX}–k_{INT}); the dike pole and k_{MIN} consequently being nearly parallel (Fig. 4a and b). The 95% confidence limits about the principal AMS directions show orthorhombic symmetry (Jelinek, 1977, 1978; Borradaile, 2001b). This confirms a weakly oblate orientation-distribution and flow-fabric. (Anisotropy parameters for individual samples are unreliable indicators of the shape of the orientation-distribution ellipsoid of minerals.) k_{MAX} might reasonably be assumed as the flow-axis, plunging gently northwards. There is no suggestion of an inverse fabric contribution from monodomainal magnetite and the large susceptibility ($k = 48{,}309 \pm 6225$ μSI) for the site favors contributions from both paramagnetic mafic silicates and oxides. Determination of AARM might therefore seem a superfluous precaution.

However, in our rocks AARM isolates the fabric contribution of oxidized titanomagnetite (compositions inferred from Curie temperatures; Dunlop and Özdemir, 1997; see Fig. 5) and magnetite to a lesser extent. The AARM fabrics do not correspond to AMS, except in a rough parallelism of symmetry planes (Fig. 4c). A_{INT} is nearly parallel to k_{MIN} and AARM foliation is almost perpendicular to AMS foliation. Clearly these oxides do not have a sufficient *anisotropy* of low-field induced susceptibility to disturb the AMS-pattern (as for example Borradaile and Gauthier, 2001) but they do reveal an incongruent oxide-subfabric. Its tensor-mean axes have very broad 95% confidence limits with an oblate fabric perpendicular to the dike-plane. We suggest the anomalous AARM fabric is due to an assemblage of complex topotactically transformed crystals formed by oxidation of TM60 and oxide-exsolution from silicates. Their orientation-distribution is feeble and its contribution to low field susceptibility is not sufficiently anisotropic to deflect the AMS-fabric from its kinematically significant orientation.

Fifteen kilometres to the south-east at Konia another homogeneous site reveals AMS patterns less readily interpreted as a consequence of magmatic flow (Fig. 5). This site is 7 km north of the E–W-trending, Southern Troodos Transform Fault Zone, a structure known to have deflected the dikes' strikes, their paleomagnetic vectors (Bonhommet et al., 1988; Borradaile, 2001a; Simonian and Gass, 1978) and their AMS fabrics (Borradaile and Gauthier, 2001) due to pervasive cataclastic shearing. This brittle behavior provides specimens free from penetrative strain (e.g. schistosity) but shears the trend of dikes leaving easily removable fragments. The AMS fabrics show the level of complication attributed elsewhere to tectonism and SD-magnetite contributions (Fig. 5a and b). AMS-foliation is notably inclined to the mean dike-trend, only k_{MAX} lying close to the mean dike-orientation, a matter that will be explained on structural grounds later. k_{MIN} axes are clearly bimodal and the tensor mean orientation of k_{MIN} lies misleadingly betwixt the two concentrations. The simple approach of sifting the data according to the mean susceptibility of the samples (e.g. Borradaile and Gauthier, 2001) fails to explain the cause of the fabric-flow plane incompatibility. One would suspect that some component of anomalous monodomainal 'inverse fabric' blended with the normal flow fabrics commonly found in this region may explain the results. However, AARM did not resolve this problem in the conventional satisfactory manner. The symmetry planes of the AARM tensor are compatible with those of the AMS tensor, but minimum and intermediate axes are swapped. Consequently, the AARM foliation is almost perpendicular to the AMS foliation, only A_{MAX} being nearly parallel to k_{MAX}, with neither convincingly close to the dike-plane (Fig. 5c). Again, the AMS contribution of the oxide-subfabric does not appear to deflect the AMS orientation-distribution but the relative magnitudes of intermediate and minimum AMS and AARM axes are incompatible. The AARM fabrics are similar to those at Panagea, whereas the AMS fabrics and deflected dike-attitudes differ (cf. Figs. 4c and 5c). One might reasonably conclude again that the AARM fabric, due to post-magmatic, sea-floor alteration responded to a late syn-crystallization stress system, similarly oriented to that at Panagea (Fig. 4c).

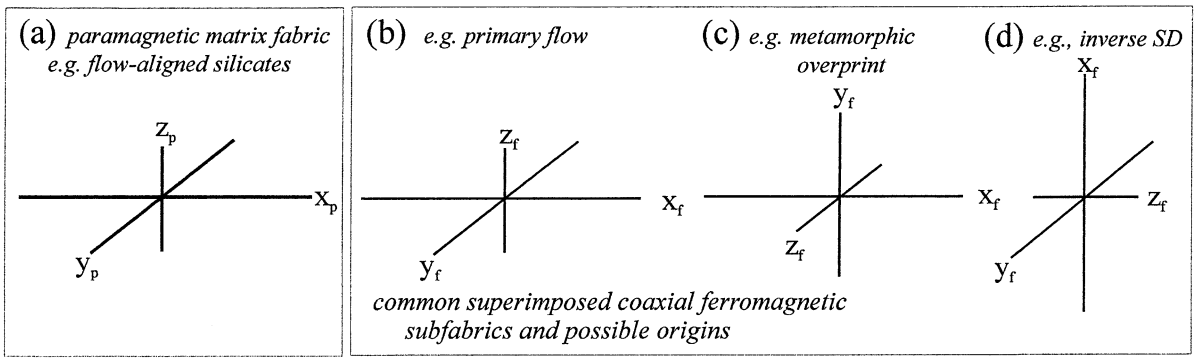

Fig. 6. (a) Magnetic sub-fabric of matrix-paramagnetic-minerals (p) with (b–d) some common possible coaxial orientations 'ferro'-magnetic subfabrics (f). The paramagnetic and ferromagnetic subfabrics both contribute to AMS, and the ferromagnetics dominate the *bulk* susceptibility though not necessarily anisotropy. However, the anisotropy of the ferromagnetics may be isolated by the AARM technique. Here only a few simple possible combinations are considered, all of which involve coaxial axes. In reality, oblique axes, and different degrees of anisotropies and bulk susceptibilities must also be considered.

3. Discussion

Most magnetic-fabric students work exclusively with AMS, due to the expense and time required for AARM. However, accessory minerals that carry remanence, particularly the iron–titanium oxides, may easily mask the AMS signal, deflecting or concealing the kinematically more significant matrix-fabric. Valid diagnostic strategies to interpret AMS fabrics that are not immediately compatible with some expected kinematic symmetry include discriminating AMS samples according to their bulk susceptibility, subarea location, or magnetic mineralogy (Rochette et al., 1991a,b; Borradaile and Henry, 1997; Lagroix and Borradaile, 2000; Borradaile and Gauthier, 2001). However, by measuring AARM the anisotropy of the remanence-bearing grains is isolated. Whereas it rarely possible to subtract this from AMS to purify the matrix fabric (Hrouda et al., 2000), one may qualitatively assess how the AMS-orientation-distribution is deflected by the accessory oxide-fabric. In mafic dikes, *bulk*-susceptibility of accessory-oxides may dwarf that of the more voluminous matrix but the AMS and AARM ellipsoids may be far from coaxial (Borradaile and Henry, 1997). This is because the weaker *anisotropy* of the oxide subfabric fails to conceal completely the AMS signature from the matrix (e.g. Borradaile, 1987). This appears to be the case in this study where the magma-flow fabric is identifiable through AMS but AARM gives a feeble, differently oriented fabric. This is understandable since the titanomaghemite accessories resulted from low-temperature oxidation of TM60. No strong preferred mineral-orientation is expected from such submarine hydrothermal metamorphism although the AARM principal orientations appear similar at both sites, suggesting that ocean-floor metamorphism may have out-lasted the shearing of dikes along the Southern Troodos Transform.

AARM is normally the preferred method of isolating the fabric. However, in this study, the *anisotropy* of the oxide subfabric is insufficient to deflect the flow-controlled AMS. However, AARM does reveal a convincingly different, weakly aligned subfabric due to Ti–Fe oxides that result from late stage sea-floor alteration, possibly post-dating the shearing of dike trends by the active portion of the Arakapas (transform) fault.

Our first recommendation is that one should consider the possibility of very weakly anisotropic magnetic-fabrics *for oxides* in ophiolite sequences. This is a general consequence of extensive sea-floor metamorphism that affects the different units (pillows, dikes, diabase, mantle sequence) to different degrees according to the degree of hydrothermal metamorphism. This depends on distance from the spreading axis, depth, and fluid-access that may be irregularly influenced by depth or proximity to transform faults. AMS contributions from TM60, titanomaghemite, ilmenite and magnetite may be very weakly anisotropic as the assemblages form by topotactic transformations with little orientations-bias. Whereas the oxides' subfabric dominates bulk susceptibility, more anisotropic mafic silicates may still express their preferred-orientation through AMS. In contrast, most previous work has attributed anomalous AMS-fabrics in ophiolites to unfavorable admixtures of single-domain and multi-domain magnetite.

Our second recommendation is that the relative (mean-susceptibility contribution) of different mineral species to the net AMS considerably influences the degree to which an anomalous subfabric is expressed, or even recognized. For simplicity, consider the most common case where competition is between paramagnetic matrix minerals and an accessory subfabric of iron oxides. Furthermore, let us assume a saturation alignment of each subfabric and a coaxial correspondence of the two subfabrics, though not always with a one-to-one correspondence of maximum, intermediate and minimum principal values. For example, consider the following diagram, in which the contribution of paramagnetic and 'ferromagnetic' subfabrics is considered vis-à-vis the overall AMS fabric (Fig. 6). The net

Table 1
possible coaxial blends of a paramagnetic matrix fabric with a ferromagnetic subfabric (see Fig. 6)

(a)	(b)	(c)				(d)
Xp	**Xf**	**Xf**	Yf	Yf	Zf	**Zf**
Yp	**Yf**	**Zf**	Xf	Zf	Xf	**Yf**
Zp	**Zf**	**Yf**	Zf	Xf	Yf	**Xf**

fabric, recognized by the AMS technique, will blend the contribution from the paramagnetic subfabric and the oxide subfabric. The AARM technique isolates the oxide subfabric but the paramagnetic fabric may normally only be inferred. According to the relative magnitudes and correspondence of axial magnitudes (P_{MAX} with F_{MAX}, or with F_{INT} or with F_{MIN}, etc.) the axes of the net AMS-ellipsoid may represent a variety of blended AMS subfabrics from different minerals and different events. Six possible coaxial blends are listed in Table 1 but only three fairly common combinations are indicated in Fig. 6. Of course, in reality the subfabric-AMS axes may not be parallel and the relative magnitudes of the axes (i.e. susceptibility magnitudes) affect the outcome. Where the *bulk* susceptibility contribution ferromagnetic subfabric is small in comparison with the *bulk* paramagnetic susceptibility of the matrix, AMS defines the orientation-distribution of matrix silicates (Fig. 6a). Conversely, if the *bulk* susceptibility of the ferromagnetic subfabric is high, the AMS will mainly indicate their alignment. The most difficult interpretations arise not just because the paramagnetic matrix and ferromagnetic accessories have similar bulk susceptibilities but because their anisotropies of low field susceptibility are also similar. Although accessory oxides dominate the bulk low-field susceptibility in this study, the net anisotropy of the complex secondary and primary oxides is too feeble to suppress the AMS-defined flow fabric.

Our third recommendation is more parochial and concerns the consideration of cataclastic deformation, here related shearing adjacent to the active portion of a transform fault. The paleomagnetic signals in these rocks are unaffected by penetrative strain. Certainly, penetrative metamorphic fabrics such as schistosity or tectonic mineral lineation, strain shadows etc., are absent. Deformation is limited to block-rotation, 'rigid-body' rotation of structural geology, in which samples are rotated with respect to an external frame of reference but internally undisturbed. It is an appreciation of the structural geologist's cataclastic foliation which enables us to understand how the dike trends and magnetic foliation have become misaligned, although the magnetic foliation still indicates magmatic flow. Dike trends shear on the outcrop sale but individual samples merely undergo block rotation so that their internal magnetic foliations lose parallelism with the walls of the sheared dikes (Fig. 7).

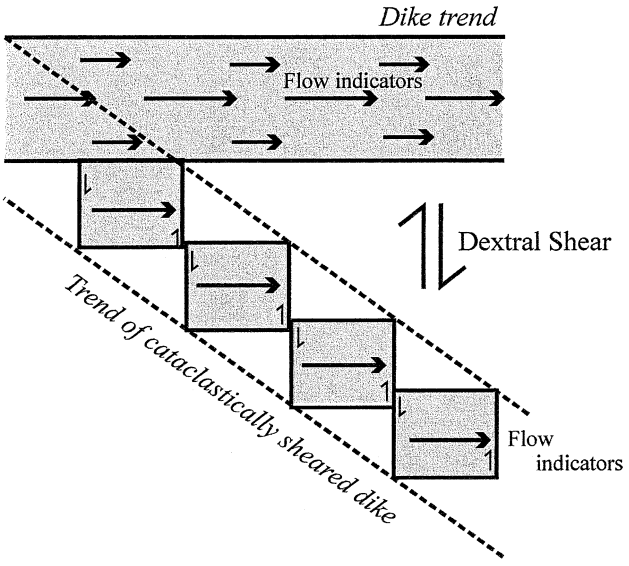

Fig. 7. Plan view sketch idealizing macroscopic or megascopic cataclastic shear on E–W fractures. The internal penetrative flow-fabric, defined magnetically, retains its orientation fairly closely, despite cataclasis.

Acknowledgements

This work was funded by the Natural Science and Engineering Research Council of Canada to Graham Borradaile. It would not have been possible without the permission and logistical support of the Geological Survey department of Cyprus, in particular their Director, Dr G. Petrides and his field Officer, Dr Ioannis Panayides. Anne Hammond is thanked for technical support in the preparation of samples. Dr Mike Stupavsky of Sapphire Instruments is thanked for ongoing support and instrumentation-development that goes far beyond the normal courtesy of commercial service.

References

Bonhommet, N., Roperch, P., Calza, F., 1988. Paleomagnetic arguments for block rotations along the Arakapas fault (Cyprus). Geology 16, 422–425.

Borradaile, G.J., 1987. Anisotropy of magnetic susceptibility: rock composition versus strain. Tectonophysics 138, 327–329.

Borradaile, G.J., 1988. Magnetic susceptibility, petrofabrics and strain—a review. Tectonophysics 156, 1–20.

Borradaile, G.J., 1994. Paleomagnetism carried by crystal inclusions: the effect of preferred crystallographic orientations. Earth Planet. Sci. Lett. 126, 171–182.

Borradaile, G.J., 2001a. Paleomagnetic vectors and tilted dikes. Tectonophysics 333, 417–426.

Borradaile, G.J., 2001b. Magnetic fabrics and petrofabrics: their orientation distributions and anisotropies. J. Struct. Geol. 23, 1581–1596.

Borradaile, G.J., Gauthier, D., 2001. Magneto-tectonic analysis of an ophiolite dike swarm. Geophys. Res. Lett. in press.

Borradaile, G.J., Henry, B., 1997. Tectonic applications of magnetic susceptibility and its anisotropy. Earth Sci. Rev. 42, 49–93.

Borradaile, G.J., Stupavsky, M., 1995. Anisotropy of magnetic susceptibility: measurement schemes. Geophys. Res. Lett. 22, 1957–1960.

Borradaile, G.J., Werner, T., 1994. Magnetic anisotropy of some phyllosilicates. Tectonophysics 235, 233–248.

Borradaile, G.J., Fralick, P.W., Lagroix, F., 1999. Acquisition of anhysteretic remanence and tensor subtraction from AMS isolates true palaeocurrent grain alignments. In: Tarling, D.H., Turner, P. (Eds.), Palaeomagnetism and Diagenesis in Sediments. Geological Society London, Special Publication 151, pp. 139–145.

Canon-Tapia, E., Walker, G.P.L., Herrero-Berevera, E., 1994. Magnetic fabric and flow direction in basaltic pahoehoe lava of Xitle Volcano, Mexico. J. Volc. Geothermal. Res. 65, 249–263.

Daly, L., Zinsser, H., 1973. Étude comparative des anisotropies de susceptibilité et d'aimantation rémanente isotherme: conséquences pour l'analyse structurale et le paléomagnétisme. Ann. Géophys. 29, 189–200.

Detrick, R., Buhl, P., Kim, I., 1990. No evidence from multi-channel reflection data for a crustal magma chamber in the MARK area, on the Mid-Atlantic Ridge. Nature 347, 61–64.

Dilek, Y., Moores, E.M., Furnes, H., 1998. Structure of modern oceanic crust and ophiolites and implications for faulting and magmatism at oceanic spreading centers. Geophys. Monograph 106, 219–265.

Dunlop, D.J., Özdemir, Ö., 1997. Rock Magnetism: Fundamentals and Frontiers. , Cambridge Studies in Magnetism. Cambridge University Press 573pp.

Elwood, B.B., 1978. Flow and emplacement direction determined for selected basaltic bodies using magnetic susceptibility anisotropy measurements. Earth Planet. Sci. Lett. 41, 254–264.

Ernst, R., Baragar, W., 1992. Evidence from magnetic fabric for the flow pattern of magma in the Mackenzie giant radiating dike swarm. Nature 356, 511–513.

Hrouda, F., 1982. Magnetic anisotropy of rocks and its application in geology and geophysics. Geophys. Surv. 5, 37–82.

Hrouda, F., Schulmann, K., 1990. Conversion of the magnetic susceptibility tensor into the orientation tensor in some rocks. Phys. Earth Planet. Inter. 63, 71–77.

Hrouda, F., Henry, B., Borradaile, G.J., 2000. Limitations of tensor subtraction in isolating diamagnetic fabrics by magnetic anisotropy. Tectonophysics 322, 303–310.

Jackson, M., 1991. Anisotropy of magnetic remanence: a brief review of mineralogical sources, physical origins, and geological applications. Pure Appl. Geophys. 136, 1–28.

Jackson, M.J., Tauxe, L., 1991. Anisotropy of magnetic susceptibility and remanence: developments in the characterization of tectonic, sedimentary, and igneous fabric. Rev. Geophys. 29, suppl., 371–376 (IUGG Report Contributions in Geomagnetism and Paleomagnetism).

Jelinek, V., 1977. The Statistical Theory of Measuring Anisotropy of Magnetic Susceptibility of Rocks and its Application. Geofyzika, Brno 88pp.

Jelinek, V., 1978. Statistical processing of anisotropy of magnetic susceptibility measured on groups of specimens. Studia geoph. et geodetica. 22, 50–62.

Jelinek, V., 1993. Theory and measurement of the anisotropy of isothermal remanent magnetization of rocks. Travaux Géophysiques 37, 124–134.

Jelinek, V., 1996. Theory and measurement of the anisotropy of isothermal remanent magnetization of rocks. Travaux Géophysiques 37, 124–134.

Knight, M., Walker, G., 1988. Magma flow directions in dikes of the Koolau Complex, Oahu, determined from magnetic fabric studies. J. Geophys. Res. 93 (B5), 4301–4319.

Kusznir, N.J., 1980. Thermal evolution of the oceanic crust: its dependence on spreading rate and effect on crustal structure. Geophys. J. R. Astronom. Soc. 61, 167–181.

Lagroix, F., Borradaile, G.J., 2000. Magnetic fabric interpretation complicated by inclusions in mafic silicates. Tectonophysics 325, 207–225.

MacDonald, W.D., Palmer, H.C., 1990. Flow directions in ash-flow tuffs: a comparison of geological and magnetic susceptibility measurements, Tshirege member (upper Bandelier Tuff), Valles Caldera, New Mexico, USA. Bull. Volcanol. 53, 45–59.

Nye, J.F., 1958. Physical Properties of Crystals. Oxford University Press 329pp.

O'Reilly, W., 1984. Rock and Mineral Magnetism. Blackie, London 220pp.

Owens, W.H., Rutter, E.H., 1978. The development of magnetic susceptibility anisotropy through crystallographic preferred orientation in a calcite rock. Phys. Earth Planet. Inter. 16, 215–222.

Palmer, H.C., MacDonald, W.D., 1999. Anisotropy of magnetic susceptibility in relation to source vents of ignimbrites: empirical observations. Tectonophysics 307, 207–218.

Potter, D.K., Stephenson, A., 1988. Single domain particles in rocks and magnetic fabric analysis. Geophys. Res. Lett. 15, 1097–1100.

Potter, D.K., Stephenson, A., 1990. Fieldimpressed anisotropies of magnetic susceptibility and remanence in minerals. J. Geophys. Res. 95, 15573–15588.

Rochette, P., 1988. Inverse magnetic fabric carbonate bearing rocks. Earth Planet. Sci. Lett. 90, 229–237.

Rochette, P., Jenatton, L., Dupuy, C., Boudier, F., Reuber, I., 1991a. Emplacement modes of basaltic dykes in the Oman ophiolite: evidence from magnetic anisotropy with reference to geochemical studies. In: Peters, T.J. (Ed.). Ophiolite Genesis and the Evolution of the Oceanic Lithosphere. Kluwer, Dordrecht, pp. 55–82.

Rochette, P., Reuber, I., Jenatton, L., Dupuy, C., Boudier, F., 1991b. Diabase dikes emplacement in the Oman ophiolite: a magnetic fabric study with reference to geochemistry. In: Peters, T. (Ed.), Ophiolite Genesis and Evolution of the Oceanic Lithosphere. Proc. Conference, Muscat, pp. 55–82.

Rochette, P., Jackson, J., Aubourg, C., 1992. Rock magnetism and the interpretation of anisotropy of magnetic susceptibility. Rev. Geophys. 30, 209–226.

Rochette, P., Aubourg, C., Perrin, M., 1999. Is this magnetic fabric normal? A review and case studies in volcanic formations. Tectonophysics 307, 219–234.

Simonian, K.O., Gass, I.G., 1978. Arakapas fault belt, Cyprus: a fossil transform fault. Geol. Soc. Am. Bull. 89, 1220–1230.

Staudigel, H., Gee, J., Tauxe, L., Varga, R., 1992. Shallow intrusive directions of sheeted dikes in the Troodos ophiolite: anisotropy of magnetic susceptibility and structural data. Geology 20, 841–844.

Staudigel, H., Tauxe, L., Gee, J., Bogaard, P., Haspels, J., Kale, G., Leenders, A., Meijer, P., Swaak, B., Tuin, M., Van Soest, M., Verdurmen, E., Zevenhuizen, A., 1999. Geochemistry and intrusive directions in sheeted dikes in the Troodos ophiolite: implications for mid-ocean ridge spreading centres. Geochem. Geophys. Geosys. [online] 1, 1999GC000001.

Stephenson, A., Sadikum, S., Potter, D., 1986. A theoretical and experimental comparison of the anistropies of magnetic susceptibility and remanence in rocks and minerals. Geophys. J. R. Astron. Soc. 84, 185–200.

Varga, R.J., Gee, J.S., Staudigal, H., Tauxe, L., 1998. Dike surface lineations as magma flow indicators within the sheeted dike complex of the Troodos Ophiolite, Cyprus. J. Geophys. Res. 103 (B3), 5241–5256.